Generation of angular momenta in fission fragments

1. Introduction
2. Model
3. Absence of correlation between the angular momenta generated in primary fission fragments
4. Saw-tooth pattern in the angular momentum as a function of fragment mass
5. Summary

T.M. Shneidman, A. Rahmatinejad , G.G. Adamian, N.V. Antonenko

Bogoliubov Laboratory of Theoretical Physics JINR

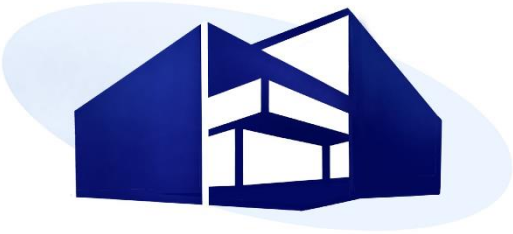

- After crossing the fission barrier, the fissioning nucleus goes into a scission configuration in which it can be treated as a dinuclear system (DNS)—system of two deformed, touching fragments.

- The DNS evolves by changing masses, charges, and deformations of the fragments. This forms the charge, mass, total kinetic energy (TKE), and neutron multiplicity distributions of fission products.

- The DNS fragments undergo angular collective motion, for example, small-amplitude vibrations of the fragments around the pole-to-pole configurations

This motion leads to striking phenomenon that even for spontaneous fission of even-even nuclei the fission fragments have rather large angular momentum [J. B.Wilhelmy, E. Cheifetz, R. C. Jared, S. G. Thompson, H. R. Bowman, and J. O. Rasmussun, PRC **5**, 2041 (1972); F. Pleasonton, R. L. Ferguson, and H. W. Schmitt, PRC **6**, 1023 (1972); A. Wolf and E. Cheifetz, PRC **13**, 1952 (1976).].

The experiments on the study of spontaneous fission of ^{252}Cf performed using GAMMASPHERE detector provided information about the correlation between average angular momenta of fission fragments and number of neutrons emitted [G. M. Ter-Akopian *et al.*, PRL **73**, 1477 (1994); PRL **77**, 32 (1996); PRC **55**, 1146 (1997); B. M. Musangu *et al.*, PRC **101**, 034610 (2020)].

First theoretical analysis of different angular vibrational modes generating angular momentum [J.R. Nix and W.J. Swiatecki, Nucl. Phys. **71**, 1 (1965)].

Quantum-mechanical consideration of the system consisting of deformed and spherical fragments [J. O. Rasmussen,W. Nörenberg, and H. J. Mang, Nucl. Phys. A **136**, 465 (1969).], and of the bending vibrational mode in the system of two deformed fragments [M. Zielinska-Pfabé and K. Dietrich, Phys. Lett. B **49**, 123 (1974).]. The quantum pumping [I.N. Mikhailov, P. Quentin, Phys.Lett.B 462, 7 (1999)]. The bending and wriggling modes were further studied in Refs. [P. O. Hess and W. Greiner, Nuovo Cimento A **83**, 76 (1984); S. Misicu, A. Sandulescu, and W. Greiner, Mod. Phys. Lett. A **12**, 1343 (1997); T.M. Shneidman et al., PRC **65**, 064302 (2002); S.G. Kadmensky et al., Bull. Russ. Acad Sci.: Phys. **79**, 879 (2015)].

The recent experimental observations [J. N. Wilson *et al.*, Nature **590**, 566 (2021)]. First, the angular correlation with different constraints imposed on one of the fragments have demonstrated an almost complete lack of correlations between the angular momenta of fission fragments. Second, the dependence of average spins on fragments mass demonstrates a saw-tooth behavior.

A variety of theoretical models have been recently proposed to address the new experimental observations including the **statistical approach** [J. Randrup and R. Vogt, PRL **127**, 062502 (2021); J.Randrup, PRC **106**, L051601 (2022); T. Døssing et al., PRC **109**, 034615 (2024)], **DFT and TD-DFT with projection** [G. F. Bertsch, T. Kawano, and L. M. Robledo, PRC **99**, 034603 (2019); P. Marevic et al., PRC **104**, L021601 (2021); A. Bulgac et al., PRL **128**, 022501 (2022)], and the models based on **time-dependent dynamics** with the collective Hamiltonian of angular vibrational modes [G. Scamps and G. Bertsch, PRC **108**, 034616 (2023); G. Scamps, PRC **109**, L011602 (2024)].

At scission, the fissioning nucleus is considered as a DNS consisting of two touching nuclei with masses $A_{1,2}$, charges $Z_{1,2}$, and quadrupole deformation parameters $\beta_{1,2}$ defined as the coefficients of expansion of the nuclear shape in spherical harmonics. Here, $A_1 + A_2 = A$, and $Z_1 + Z_2 = Z$, where Z and A are the charge and mass of the fissioning nucleus, respectively.

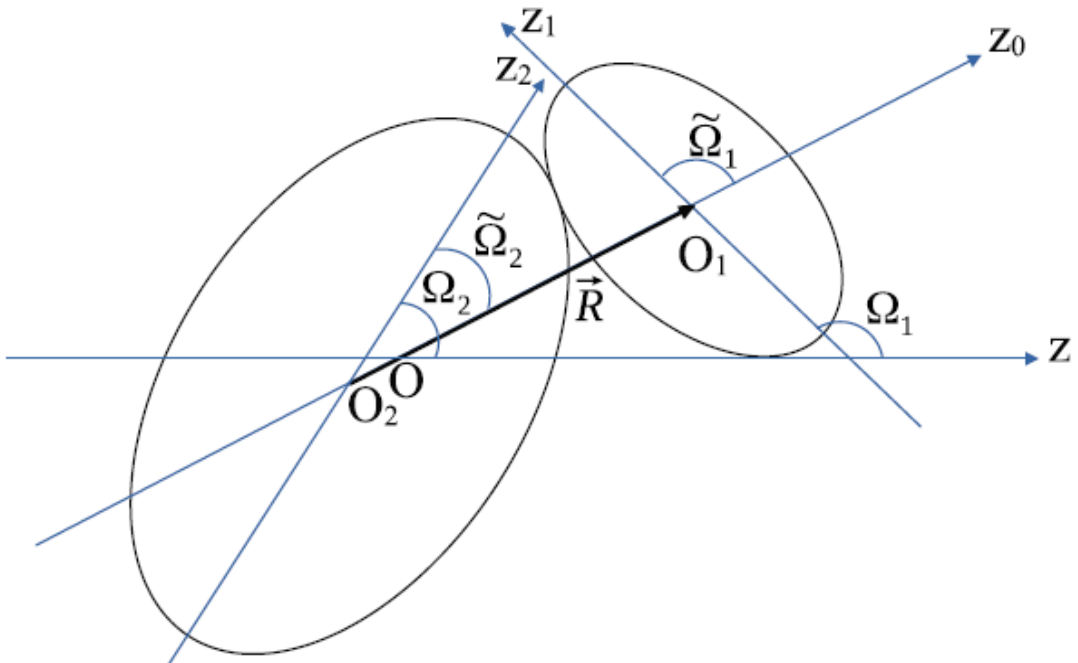

laboratory system is defined by the Euler angles $\Omega_0 = (\phi_0, \theta_0, 0)$

The orientations of intrinsic systems of the fragments O_1z_1 and O_2z_2 with respect to the laboratory system are $\Omega_{1,2} = (\phi_{1,2}, \theta_{1,2}, 0)$ and with respect to the body-fixed system are $\tilde{\Omega}_{1,2} = (\gamma_{1,2}, \varepsilon_{1,2}, 0)$.

The Hamiltonian of the DNS at fixed mass (charge) asymmetry is written as

$$H = \frac{\hbar^2 \hat{I}_0^2}{2\mu R_m^2} + \frac{\hbar^2 \hat{I}_1^2}{2\Im_1} + \frac{\hbar^2 \hat{I}_2^2}{2\Im_2} + V(R_m, \Omega_0, \Omega_1, \Omega_2), \quad (1)$$

where $R_m = R_m(\Omega_0, \Omega_1, \Omega_2) = R_m(\tilde{\Omega}_1, \tilde{\Omega}_2)$ is the distance corresponding to the touching configuration of the fragments for a given orientation. The kinetic energy describes the rotation of the individual fragments and their relative rotation with respect to the laboratory system. In Eq. (1), $\Im_{1,2}$, and $\Im_R = \mu R_m^2$ are the moments of inertia of the fragments and of the relative rotation, respectively. The reduced mass of the DNS is $\mu = m_0 A_1 A_2 / A$, where m_0 is the nucleon mass. The moments of inertia of the fragments are taken in the rigid body limit as

$$\Im_i = \int d\tau \left(x_i^2 + z_i^2\right) \rho_i(\mathbf{r}) = \int d\tau \left(y_i^2 + z_i^2\right) \rho_i(\mathbf{r})$$

$$\approx \frac{2}{5} m_0 A_i R_i^2 \left(1 + \sqrt{\frac{5}{16\pi}} \beta_i + \frac{20}{7\pi} \beta_i^2 + \frac{5\sqrt{5}}{8\pi^{3/2}} \beta_i^3 + \cdots\right), \quad (i = 1, 2).$$

The angular momentum operators are explicitly written in terms of Euler angles as

$$\hat{I}_i^2 = -\left(\frac{1}{\sin\theta_i} \frac{\partial}{\partial\theta_i} \sin\theta_i \frac{\partial}{\partial\theta_i} + \frac{1}{\sin^2\theta_i} \frac{\partial^2}{\partial\phi_i^2} \right), \quad (i = 0, 1, 2).$$

The eigenstates of kinetic energy operator are written in terms of tripolar spherical harmonics

$$[i_0 \times [i_1 \times i_2]_{i_{12}}]_{(I,M)} \equiv \left[Y_{i_0}(\Omega_0) \times \left[Y_{i_1}(\Omega_1) \times Y_{i_2}(\Omega_2) \right]_{i_{12}} \right]_{(I,M)}$$

$$= \sum_{m_0 m_1 m_2 m_{12}} C^{IM}_{i_0 m_0, i_{12} m_{12}} C^{i_{12} m_{12}}_{i_1 m_1, i_2 m_2} Y_{i_0 m_0}(\Omega_0) Y_{i_1 m_1}(\Omega_1) Y_{i_2 m_2}(\Omega_2).$$

In the case of even-even spontaneously fissioning nucleus considered $I = M = 0$ which leads to $i_{12}=i_0$

$$V(\tilde{\Omega}_1, \tilde{\Omega}_2) = V_C(R_m(\tilde{\Omega}_1, \tilde{\Omega}_2), \tilde{\Omega}_1, \tilde{\Omega}_2) + V_N(R_m(0,0), 0, 0),$$

V_N is taken for pole-pole orientation

The Coulomb interaction is calculated in terms of multipole expansion as

$$V_C = \sum_{\lambda_1 \lambda_2} V_{\lambda_1,\lambda_2}(\beta_1, \beta_2)\left[Y_{\lambda_1}(\tilde{\Omega}_1) \times Y_{\lambda_2}(\tilde{\Omega}_2)\right]_{(\lambda_1+\lambda_2\ 0)},$$

$$V_{\lambda_1,\lambda_2}(\beta_1, \beta_2) = (-1)^{\lambda_2} \sqrt{\frac{(4\pi)^2(2\lambda_1 + 2\lambda_2)!}{(2\lambda_1 + 1)!(2\lambda_2 + 1)!}} \times \frac{Q^{(1)}_{\lambda_1}(\beta_1) Q^{(2)}_{\lambda_2}(\beta_2)}{R_m^{\lambda_1+\lambda_2+1}(\tilde{\Omega}_1, \tilde{\Omega}_2)}, \quad (6)$$

where

$$Q^{(i)}_{\lambda}(\beta_i) = \sqrt{\frac{4\pi}{2\lambda + 1}} \int \rho_i(\mathbf{r}_i) r_i^{\lambda} Y_{\lambda 0}(\theta, \phi) d\mathbf{r}_i \quad (7)$$

are multipole moments of the fragments ($i = 1, 2$).

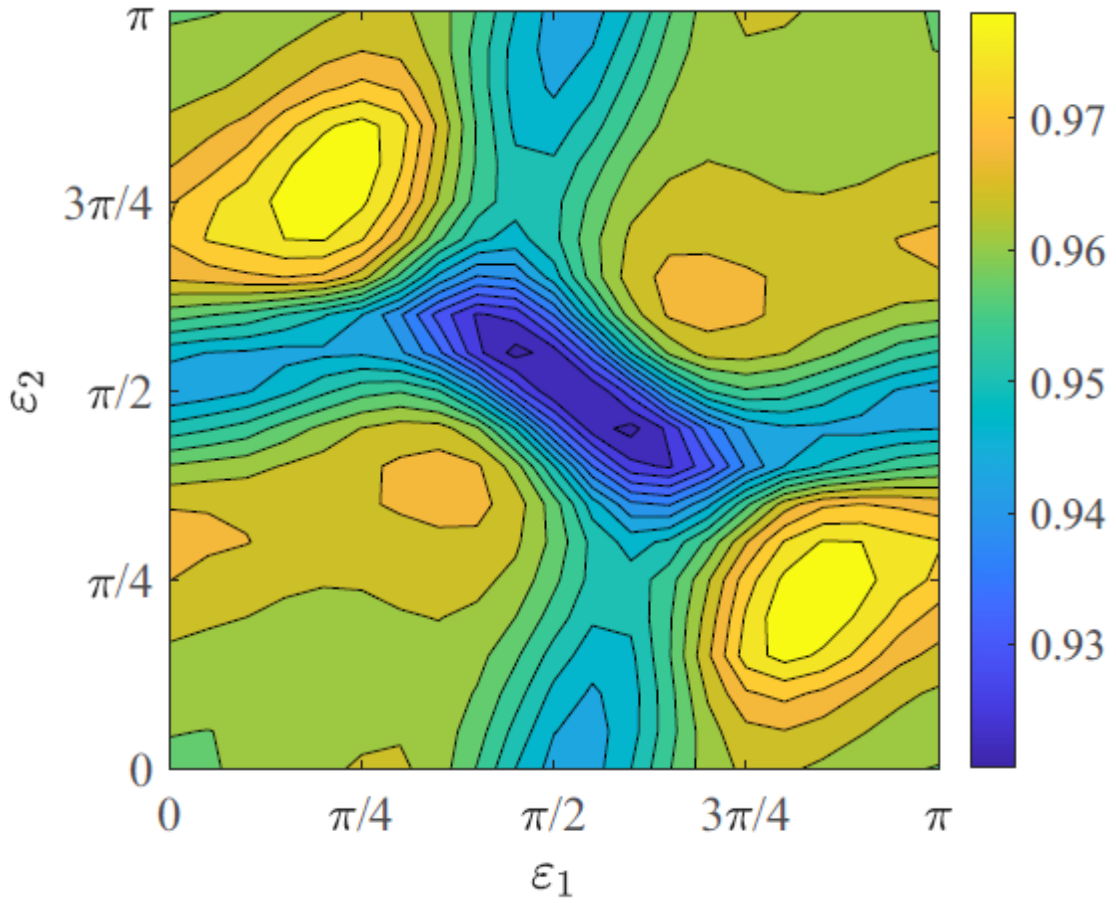

FIG. 2. The ratio of exact interaction potential at touching configuration for different orientations to the approximated interaction potential in Eq. (5). The azimuthal angles are taken as zero $\gamma_1 = \gamma_2 = 0$. The calculations are performed for the DNS ^{102}Zr($\beta_{\mathrm{Zr}} = 0.7$)+ ^{150}Ce($\beta_{\mathrm{Ce}} = 0.7$).

The potential energy is transformed to the laboratory system using the expression

$$\left[Y_{\lambda_1}(\tilde{\Omega}_1) \times Y_{\lambda_2}(\tilde{\Omega}_2)\right]_{(\lambda_0 0)}$$
$$= \sqrt{4\pi}\left[Y_{\lambda_0}(\Omega_0) \times \left[Y_{\lambda_1}(\Omega_1) \times Y_{\lambda_2}(\Omega_2)\right]_{\lambda_0}\right]_{(00)}.$$

$$H = \frac{\hbar^2 \hat{l}_0^2}{2\mu R_m^2(\tilde{\Omega}_1, \tilde{\Omega}_2)} + \frac{\hbar^2 \hat{l}_1^2}{2\Im_1} + \frac{\hbar^2 \hat{l}_2^2}{2\Im_2} + \sqrt{4\pi} \sum_{\lambda_1, \lambda_2} V_{\lambda_1, \lambda_2}\left[(\lambda_1 + \lambda_2) \times [\lambda_1 \times \lambda_2]_{(\lambda_1+\lambda_2)}\right]_{(00)},$$

$$\frac{1}{\mu R_m^2(\tilde{\Omega}_1, \tilde{\Omega}_2)} = \frac{1}{\mu R_m^2(0,0)}\left[1 + \sqrt{4\pi} \sum_{\lambda_0, \lambda_1, \lambda_2} R^{(2)}_{\lambda_0, \lambda_1, \lambda_2}\left[\lambda_0 \times [\lambda_1 \times \lambda_2]_{\lambda_0}\right]_{(00)}\right]$$

For spontaneous fission of even-even nucleus, the eigenstates of H are expressed as

$$\psi_n = \sum_{i_0 i_1 i_2} a^{(n)}_{i_0 i_1 i_2} \left[i_0 \times [i_1 \times i_2]_{i_0} \right]_{(00)}.$$

Since the fission fragments are assumed to be reflection-symmetric, the values of $i_{1,2}$ are even. Therefore, i_0 is also even, $|i_1\text{-}i_2| \leq i_0 \leq |i_1+i_2|$. The value of $|a^{(n)}_{i_0 i_1 i_2}|^2$ gives the probability of angular momenta $i_{1,2,0}$.

Neglecting the coupling between the angular vibrations of the fragments, the excitation spectrum of the angular motion is approximately written as

$$E_{n_1,n_2,\bar{K}} = \hbar\omega_1(2n_1 + |\bar{K}| + 1) + \hbar\omega_2(2n_2 + |\bar{K}| + 1).$$

$$\omega_i = \sqrt{C_i/\Im_{b,i}}, \quad (i = 1, 2),$$

$$\Im_{b,i} = (1/\Im_0 + 1/\Im_i)^{-1} \approx \Im_i$$

the ground states with $n_1 = n_2 = \bar{K} = 0$.

$$E_{1,0,0} = 2\hbar\omega_1, E_{0,1,0} = 2\hbar\omega_2, \text{ and } E_{0,0,1} = \hbar(\omega_1 + \omega_2).$$

We associate the ground states with $n_1 = n_2 = \bar{K} = 0$. The first group consists of states with energies $E_{1,0,0} = 2\hbar\omega_1$, $E_{0,1,0} = 2\hbar\omega_2$, and $E_{0,0,1} = \hbar(\omega_1 + \omega_2)$.

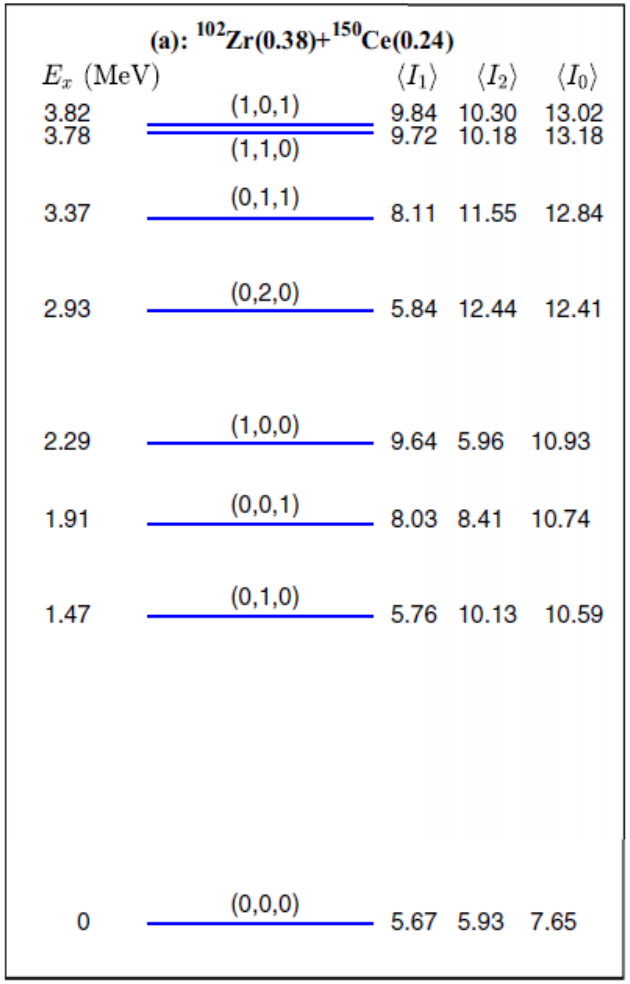

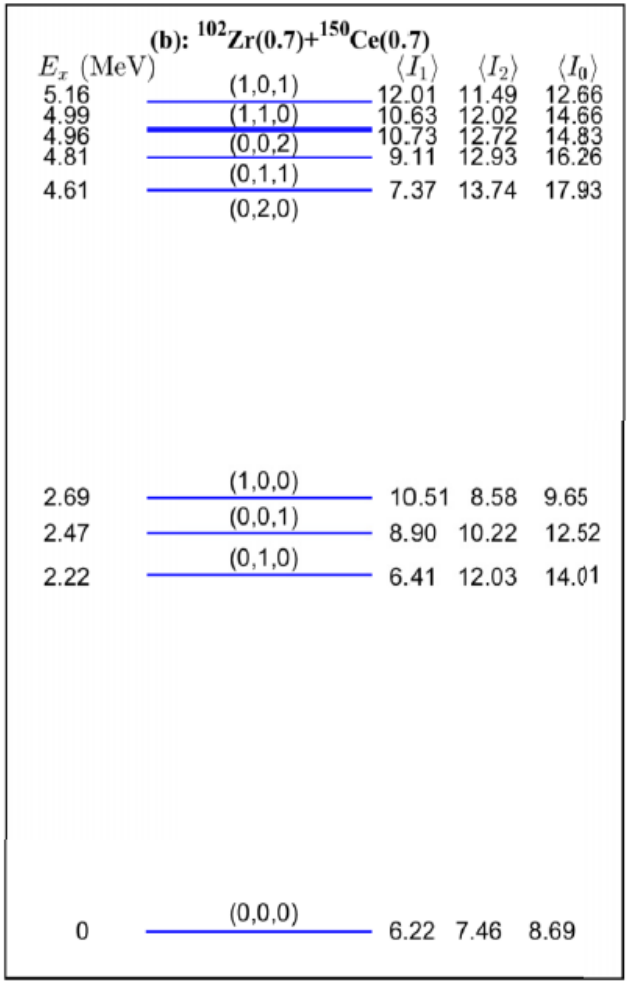

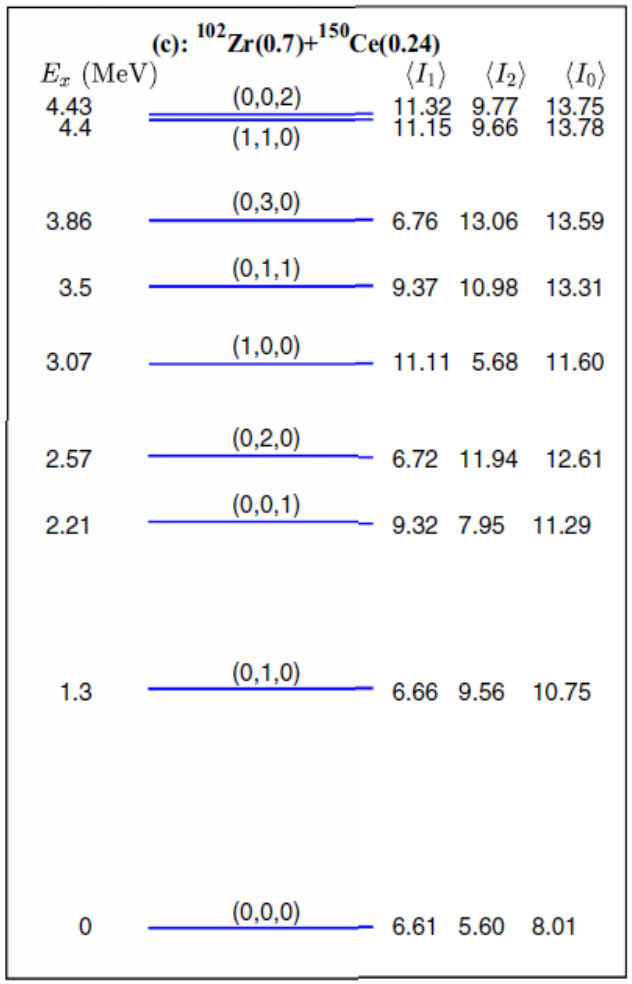

the distribution of K values for any particular low-lying state should be peaked around approximate value 0, 1, 2 . . . characterizing this state

$$\left[Y_{i_0}(\Omega_0)\times\left[Y_{i_1}(\Omega_1)\times Y_{i_2}(\Omega_2)\right]_{i_0}\right]_{(00)}=\frac{(-1)^{i_0}}{\sqrt{4\pi}}\sum_K C^{i_0 0}_{i_1 K i_2 -K}Y_{i_1 K}(\tilde{\Omega}_1)Y_{i_2 -K}(\tilde{\Omega}_2),$$

$$Y_{i_1 K}(\tilde{\Omega}_1)Y_{i_2 -K}(\tilde{\Omega}_2)=\sum_{i_0}(-1)^{-i_0}\sqrt{4\pi}C^{i_0 0}_{i_1 K i_2 -K}\left[Y_{i_0}(\Omega_0)\times\left[Y_{i_1}(\Omega_1)\times Y_{i_2}(\Omega_2)\right]_{i_0}\right]_{(00)},$$

$$P_n(K)=2\sum_{i_0 i_1 i_2}\left|a^{(n)}_{i_0 i_1 i_2}\right|^2\left|C^{i_0 0}_{i_1 K i_2 -K}\right|^2.$$

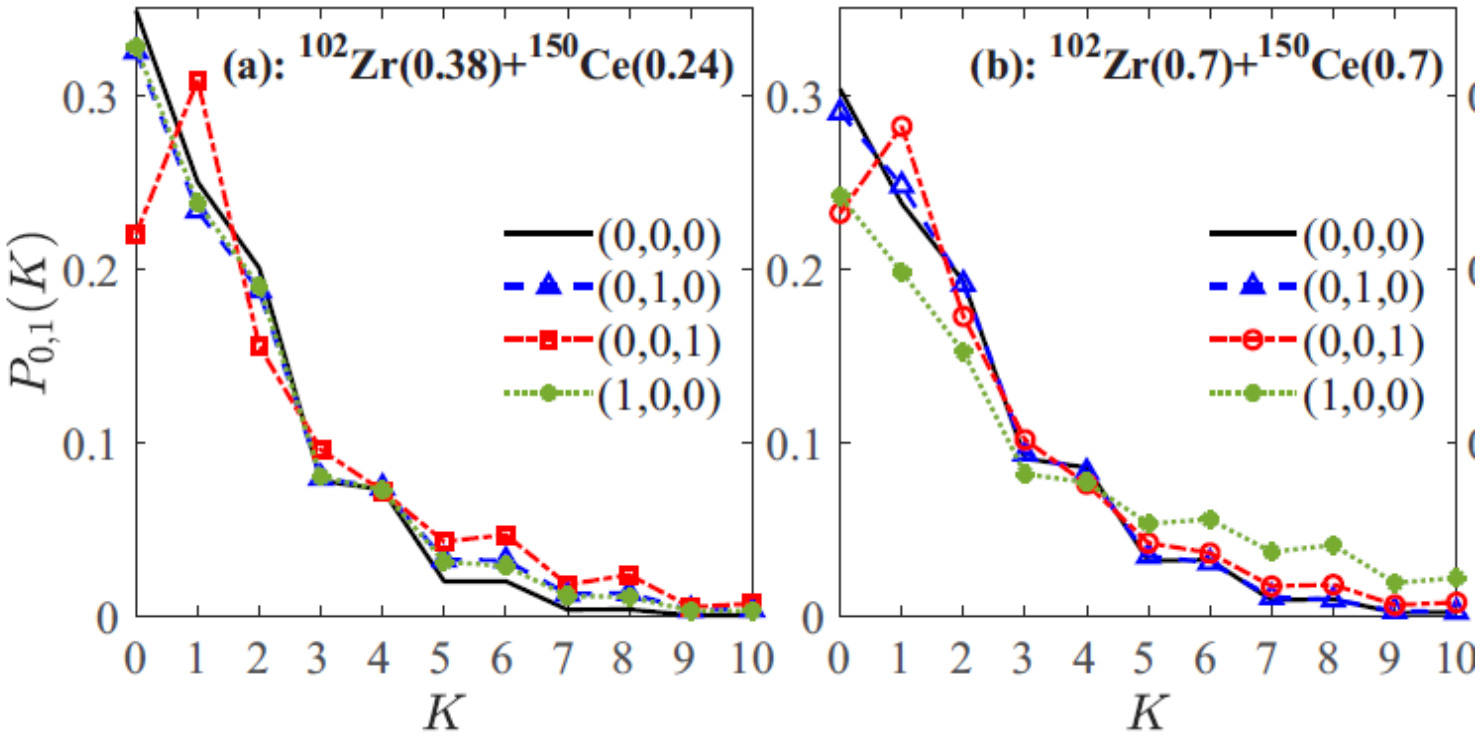

We calculate average angular momentum of the first fragment with a constraint that the angular momentum of the second fragment is larger than $I_{\min} = 0, 2, 4, \ldots$.

$$\langle I_1 \rangle_n = \left[\sum_{i_0, i_1, i_2 \geqslant I_{min}} \left| a^{(n)}_{i_0 i_1 i_2} \right|^2 i_1 (i_1 + 1) \right]^{1/2} .$$

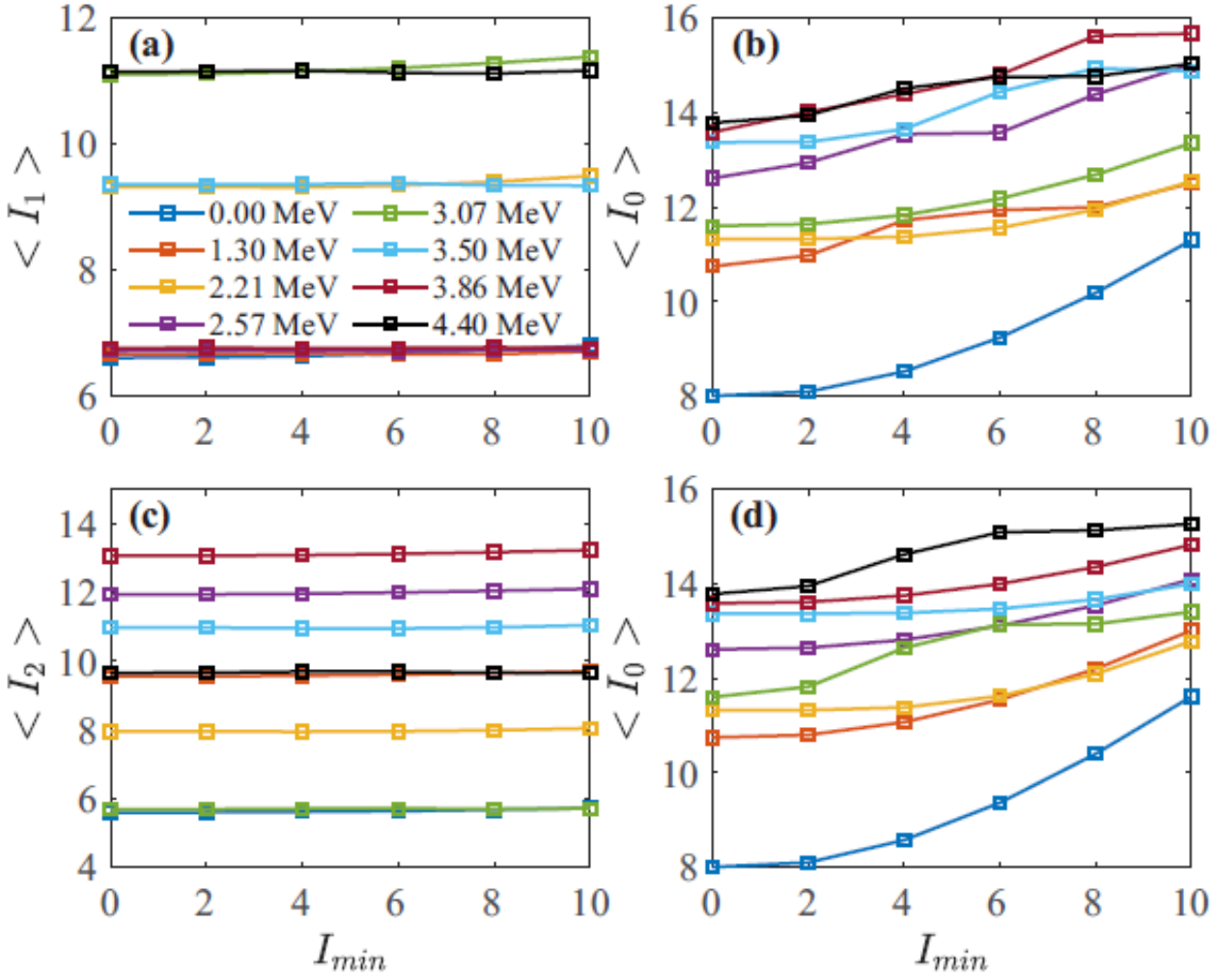

FIG. 6. (a,b) The values of $\langle I_{1,0} \rangle$ for the lowest states of angular vibration with indicated energies in the ^{102}Zr($\beta = 0.7$) + ^{150}Ce($\beta = 0.24$) system with various constraints on the angular momentum of the second fragment $I_2 \geqslant I_{min}$. (c,d) The same, but for $\langle I_{2,0} \rangle$ with constraints $I_1 \geqslant I_{min}$.

The absence of correlations becomes even more distinct if one plots the probability distribution of I_i for different constraints imposed on the angular momentum of the second fragment. It is evident that the corresponding curves are to a large extent identical, indicating the independence of angular momenta of two fragments.

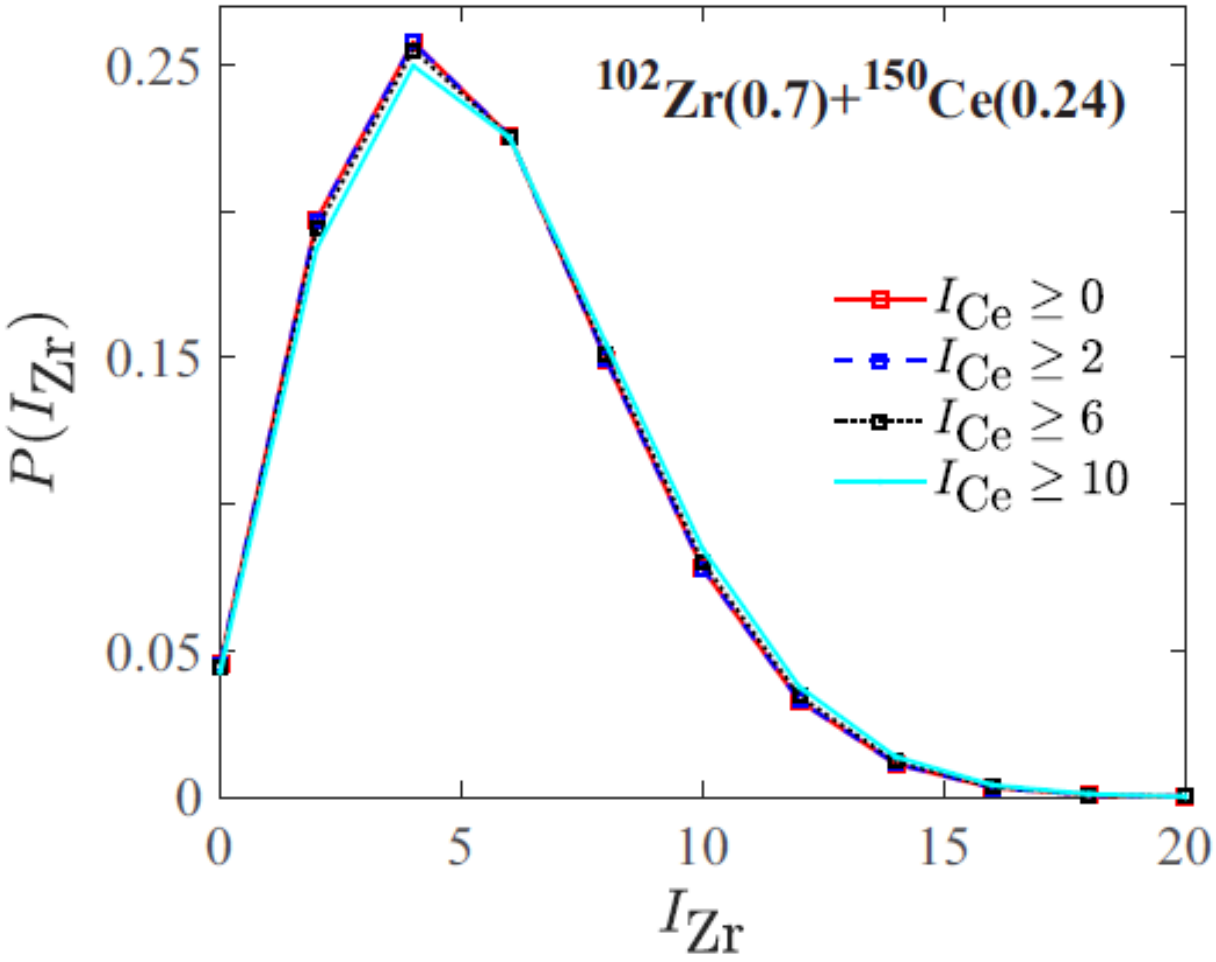

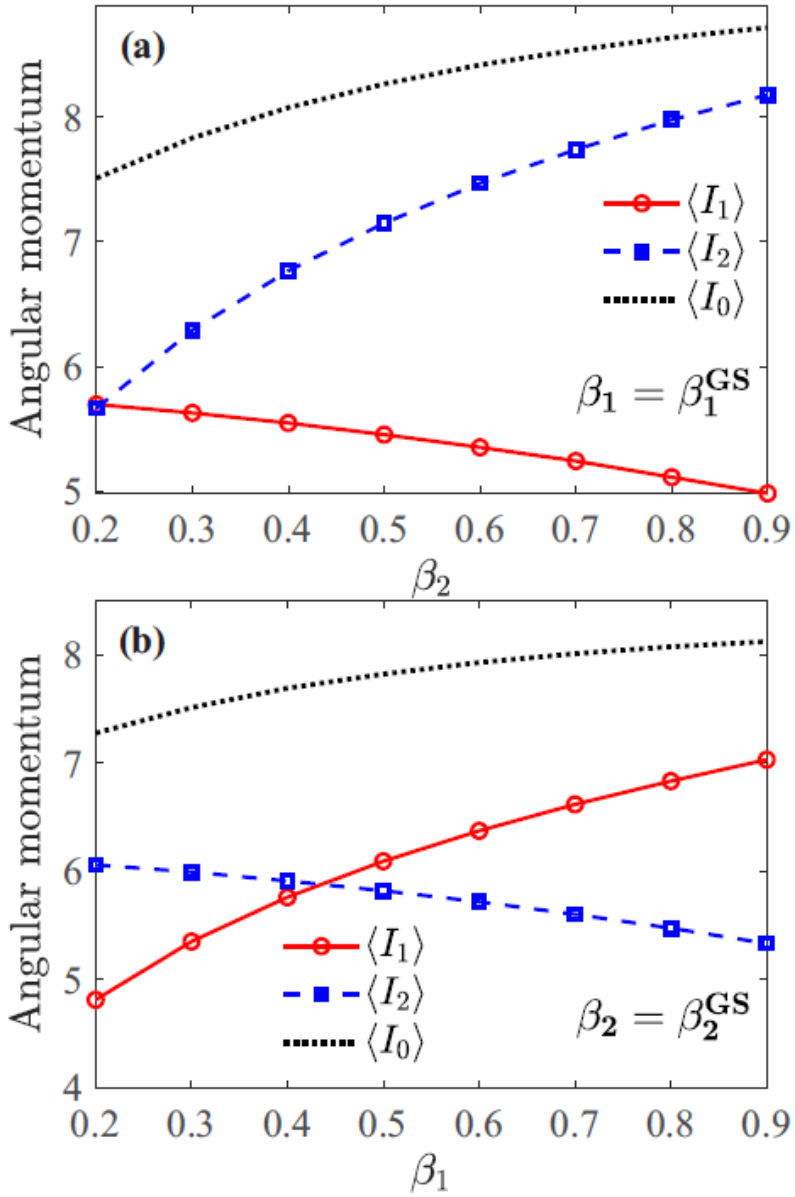

FIG. 8. Average angular momenta $\langle I_0 \rangle$, $\langle I_1 \rangle$ and $\langle I_2 \rangle$ for $^{102}\mathrm{Zr}(\beta_1) + {}^{150}\mathrm{Ce}(\beta_2)$ as a function of deformation β_2 at $\beta_1 = \beta_1^{\mathrm{GS}}$ (a), and as a function of deformation β_1 at $\beta_2 = \beta_2^{\mathrm{GS}}$ (b).

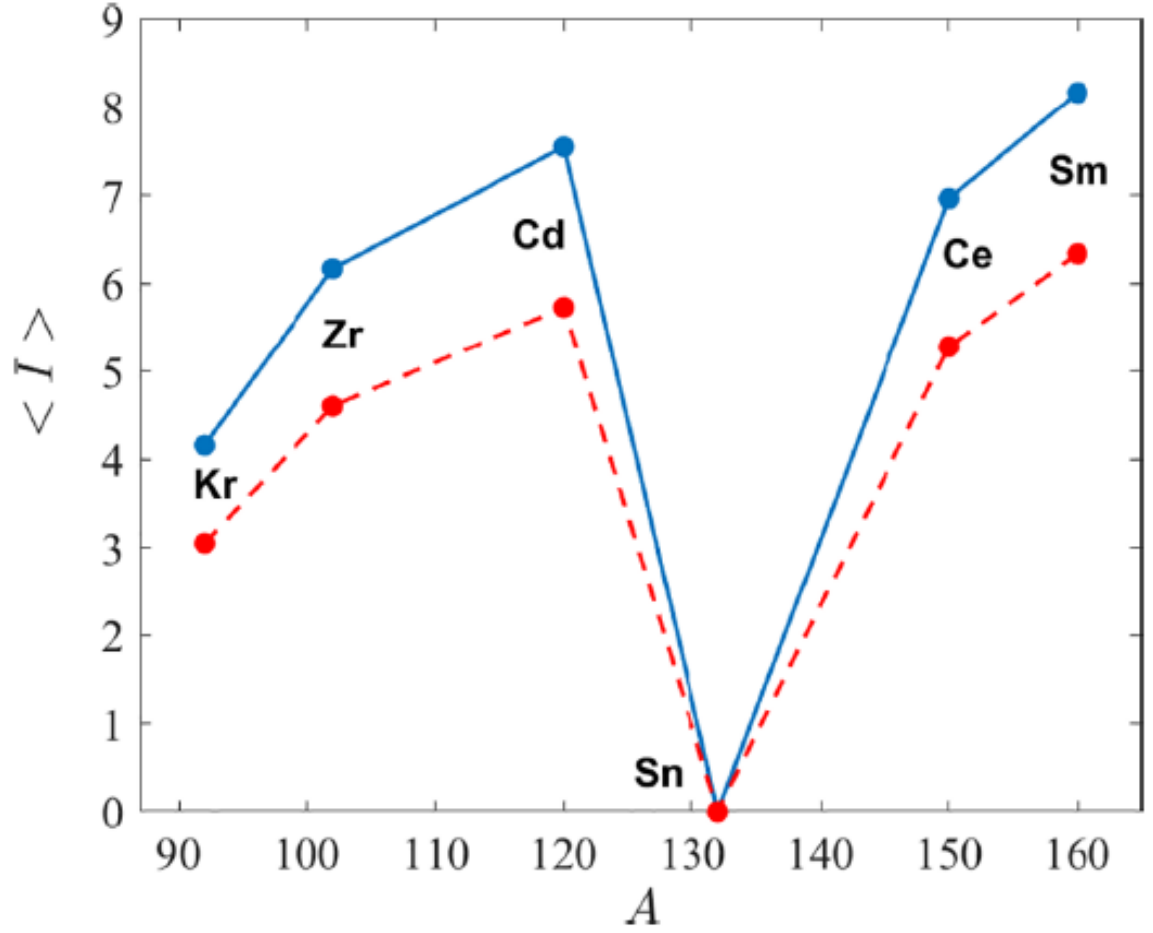

FIG. 9. Average angular momentum as a function of fragment mass calculated for the ^{92}Kr($\beta = 0.24$)+ ^{160}Sm($\beta = 0.8$), ^{102}Zr($\beta = 0.6$)+ ^{150}Ce($\beta = 0.5$), and ^{120}Cd($\beta = 0.8$)+ ^{132}Sn($\beta = 0$) systems resulting from spontaneous fission of ^{252}Cf. The calculated points obtained with rigid body moments of inertia are connected by solid line and those obtained with moments of inertia of 30% of the rigid body value are connected by dashed line.

$$\langle \nu_i \rangle \approx \frac{1}{S_n}\left(E_i^{\mathrm{def}}(Z_i, A_i, \beta_i) + \frac{A_i}{A_1 + A_2} E^* \right) \quad (i = 1, 2),$$

$$\langle TKE \rangle = V_C(Z_{1,2}, A_{1,2}, \beta_{1,2}, R_m) + V_N(Z_{1,2}, A_{1,2}, \beta_{1,2}, R_m).$$

DNS	β_1	β_2	E^{def} (MeV)	E^* (MeV)
^{92}Kr + ^{160}Sm	0.24	0.8	23.80	0.28
^{102}Zr + ^{150}Ce	0.6	0.5	9.05	4.94
^{120}Cd + ^{132}Sn	0.8	0.0	18.87	4.53

For ^{102}Zr and ^{150}Ce the experiment yields $<I_{Zr}>$ = (5.84 ± 0.13) and $<I_{Ce}>$ = (9.12 ± 0.35) which is in satisfactory agreement with values obtained with the rigid body moments of inertia $<I_{Zr}>$ = 6.16 and $<I_{Ce}>$ = 7.2. For ^{132}Sn the experiment results in $<I_{Sn}>$ = (3.95 ± 0.68), while the calculations give $<I_{Sn}>$ = 0. At scission ^{132}Sn is populated in the states with different deformations due to the polarization effects of the nuclear interaction that increases the average angular momentum.

Summary

- The model was proposed for quantum mechanical treatment of angular motion in the system consisting of two fission fragments at touching.
- Unlike the bending/wriggling scenario, this motion can be considered as small-amplitude independent vibrations of fragments around pole-to-pole configuration.
- Angular momentum generated by the vibrations is balanced by the relative rotation of DNS fragments.
- The model allows us to explain the absence of correlation between the angular momenta generated in primary fission fragments.
- The distribution of projection of angular momenta of the fragments on the separation axis is peaked around either $K = 0$ or $K = 1$, but it extends well to $K \approx 4$.
- The model explains the saw-tooth pattern in the angular momentum as a function of fragment mass.